899169

MODELING AND SIMULATION OF INVERTER-FED INDUCTION MOTORS USING THE NATURAL ABC FRAME OF REFERENCE

T.M. Hijazi, Member
M.A. Alhamadi, Student Member
A.A. Arkadan, Member
N.A. Demerdash, Senior Member

ECE Dep., Clarkson University, Potsdam, N.Y. 13676

Abstract - A time-domain equivalent network model, in the natural ABC frame of reference, for computer-aided prediction of the performance of dc source-inverter fed induction motor systems is presented and verified experimentally. The choice of this frame of reference for stator representation facilitates the integration of the machine and the electronic dc source-inverter models into one global equivalent network for the entire system. This model is most suited for the propulsion and actuation class of drives in which induction motors may serve as substitutes for brushless dc motors as prime movers. The model was used to simulate the performance of a 204 V, 1/3 hp, 60 Hz, 4-pole induction motor-inverter system, which was verified by corresponding test results obtained in the laboratory. Furthermore, the model was applied to a 440 v, 15 hp, 60 Hz, 8-pole induction motor-inverter system for purposes of evaluating the effects of 180° e and 120° e inverter conduction periods on the currents and torque profiles of the drive system.

INTRODUCTION

In numerous papers on electromechanical actuation and propulsion applications, electronically-commutated permanent magnet brushless dc motors were used as prime-movers for such drive systems [1-5]. The design and analysis of several of these systems were carried out by use of a computer-aided approach, in which the performance characteristics of the machine and its associated electronic power conditioning equipment were obtained using equivalent circuit-network graph theory techniques [6,7]. In that approach, the machine parameters can be computed from magnetic field solutions using the combined finite element-energy perturbation methods as was demonstrated in reference [8]. The natural ABC frame of reference was always adhered to, in modeling the armature windings of such machines which must directly be interfaced with the electronic power conditioners [4-7]. This means that the natural ABC currents flowing in any power conditioner are also the state variables used in representing the machine dynamics, and hence its interactions with the power conditioner to which it is interfaced.

In this present work, a computer-aided model was developed as a tool to enable the future investigation of the advantages and drawbacks of the possible replacement of the permanent magnet motor by an induction machine of the same rating as the prime-mover in such propulsion and actuation drives. The assumption is that the topology of the power conditioner would remain very similar to that used with permanent magnet machines associated with brushless dc systems. Accordingly, the present modeling effort centers on the simulation of a dc source-power conditioner (inverter) induction motor system such as shown in Figure (1). Here, the nature of the power source is the same as that in previous brushless dc machine systems [1-6].

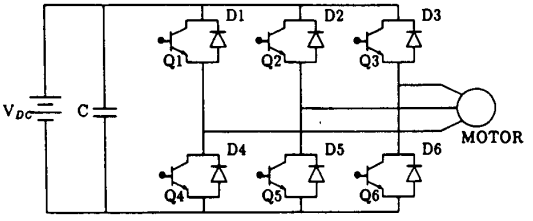

SCHEMATIC OF INVERTER-FED INDUCTION MOTOR SYSTEM
Figure (1)

By and large, previous efforts to model inverter-fed induction motors were carried out using variations of the DQO frame of reference [9,10]. These models inherently are formulated in terms of "synthetic" direct and quadrature currents, and are based on the assumption of flux distributions around the airgap and armature circumferences that are purely sinusoidal in nature. This precludes a sufficiently rigorous account of the effects of space harmonics resulting from winding layouts, and rotor as well as stator magnetic circuit geometries, that is slotting, fractional slot windings, etc. This is unlike the natural ABC frame of reference approach which is formulated in terms of the "physical" ABC armature currents, and which was adopted by these authors in modeling of brushless dc and other permanent magnet machines [4,5,11,12]. Furthermore, in the natural ABC frame of reference approach, all the effects of the significant space harmonics on machine parameters can be accounted for. Accordingly, the present model was developed with a view to enable one to include such effects in future studies of such dc source-inverter fed induction machine systems of the type shown in Figure (1). This approach would lead to a comparison on a sound basis between equivalent permanent magnet versus induction type machines in drive systems for propulsion and actuation applications.

Accordingly, a natural ABC frame of reference time-domain equivalent network model for study of the performance characteristics of dc source-inverter fed induction motors was developed, as will be detailed below. However, the model was applied here only for purposes of showing its compatibility with conventional equivalent circuits of induction motors, in which no harmonic

CH2781-3/89/0000-0527 $1.00 © 1989 IEEE

fluxes higher than the fundamental are considered. The validity of the model was verified experimentally by comparing its simulation results with actual test data on a 204 v, 1/3 hp, 60 Hz, 4-pole induction motor-inverter system, where very good agreement was achieved between computer generated and experimental data. Furthermore, the model was used in comparing the performance of a 440 V, 15 hp, 60 Hz, 8-pole induction motor when operated from inverters with 180° e and 120° e inverter conduction periods. The results are in accordance with known trends about induction motor performance under these two conduction periods, which is further evidence of the soundness of the modeling approach presented here.

EQUIVALENT NETWORK MODEL OF THE DC SOURCE-INVERTER FED INDUCTION MOTOR SYSTEM IN ABC FRAME OF REFERENCE

An idealized three phase induction motor shown in Figure (2) can be represented schematically by the equivalent coils (windings) of Figure (3). Windings, A, B, and C, Figure (2), represent the stator phase windings, and windings, a, b, and c represent the rotor's three phase windings. The three balanced stator (and rotor) phases are 120 electrical degrees apart, respectively, and the angular position of the rotor, σ, is defined as the angle between the A-axis of the stator and the a-axis of the rotor.

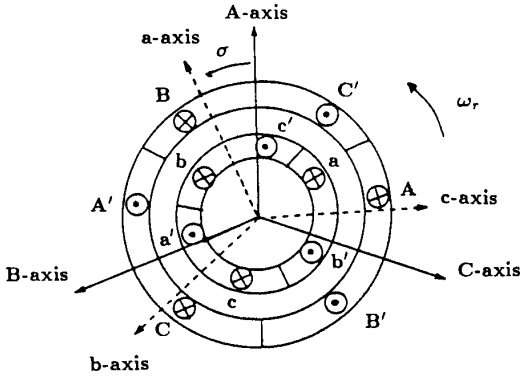

SCHEMATIC OF 3-PHASE INDUCTION MACHINE
Figure (2)

The differential equations governing the dynamic behavior of the induction machine in the ABC frame of reference can be expressed as follows:

$$\left[\begin{array}{c} v_A \\ v_B \\ v_C \\ \hline v_a \\ v_b \\ v_c \end{array}\right] = \left[\begin{array}{ccc|ccc} r_A & 0 & 0 & 0 & 0 & 0 \\ 0 & r_B & 0 & 0 & 0 & 0 \\ 0 & 0 & r_C & 0 & 0 & 0 \\ \hline 0 & 0 & 0 & r_a & 0 & 0 \\ 0 & 0 & 0 & 0 & r_b & 0 \\ 0 & 0 & 0 & 0 & 0 & r_c \end{array}\right] \left[\begin{array}{c} i_A \\ i_B \\ i_C \\ \hline i_a \\ i_b \\ i_c \end{array}\right] +$$

$$\left[\begin{array}{ccc|ccc} L_{AA} & L_{AB} & L_{AC} & L_{Aa} & L_{Ab} & L_{Ac} \\ L_{BA} & L_{BB} & L_{BC} & L_{Ba} & L_{Bb} & L_{Bc} \\ L_{CA} & L_{CB} & L_{CC} & L_{Ca} & L_{Cb} & L_{Cc} \\ \hline L_{aA} & L_{aB} & L_{aC} & L_{aa} & L_{ab} & L_{ac} \\ L_{bA} & L_{bB} & L_{bC} & L_{ba} & L_{bb} & L_{bc} \\ L_{cA} & L_{cB} & L_{cC} & L_{ca} & L_{cb} & L_{cc} \end{array}\right] \frac{d}{dt} \left[\begin{array}{c} i_A \\ i_B \\ i_C \\ \hline i_a \\ i_b \\ i_c \end{array}\right] +$$

$$\omega_r \left\{ \frac{d}{d\sigma} \left[\begin{array}{ccc|ccc} L_{AA} & L_{AB} & L_{AC} & L_{Aa} & L_{Ab} & L_{Ac} \\ L_{BA} & L_{BB} & L_{BC} & L_{Ba} & L_{Bb} & L_{Bc} \\ L_{CA} & L_{CB} & L_{CC} & L_{Ca} & L_{Cb} & L_{Cc} \\ \hline L_{aA} & L_{aB} & L_{aC} & L_{aa} & L_{ab} & L_{ac} \\ L_{bA} & L_{bB} & L_{bC} & L_{ba} & L_{bb} & L_{bc} \\ L_{cA} & L_{cB} & L_{cC} & L_{ca} & L_{cb} & L_{cc} \end{array}\right] \right\} \left[\begin{array}{c} i_A \\ i_B \\ i_C \\ \hline i_a \\ i_b \\ i_c \end{array}\right] \quad (1)$$

where $\omega_r = \dot{\sigma} = (1 - s)\omega_s$. Here, the instantaneous rotor speed, ω_r, and the synchronous speed, ω_s, are in electrical rad/s, and the slip of the motor, s is in per unit.

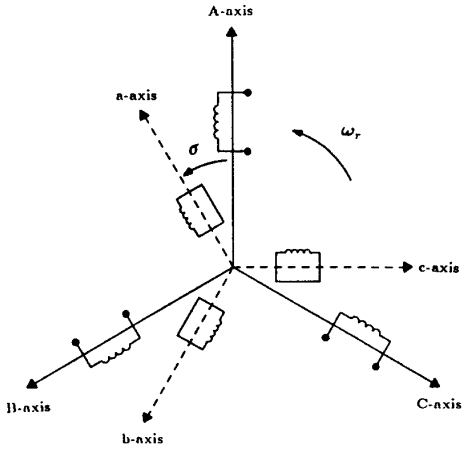

SCHEMATIC REPRESENTATION OF INDUCTION MACHINE WINDINGS
Figure (3)

Equation (1) can be rewritten in a compact matrix formulation as follows:

$$\left[\begin{array}{c} \underline{V_{ABC}} \\ \hline \underline{V_{abc}} \end{array}\right] = \left[\begin{array}{c|c} \underline{\mathrm{R}_{ss}} & \underline{0} \\ \hline \underline{0} & \underline{\mathrm{R}_{rr}} \end{array}\right] \left[\begin{array}{c} \underline{I_{ABC}} \\ \hline \underline{I_{abc}} \end{array}\right] +$$

$$\left[\begin{array}{c|c} \underline{\mathrm{L}_{ss}} & \underline{\mathrm{L}_{sr}} \\ \hline \underline{\mathrm{L}_{sr}^T} & \underline{\mathrm{L}_{rr}} \end{array}\right] \frac{d}{dt} \left[\begin{array}{c} \underline{I_{ABC}} \\ \hline \underline{I_{abc}} \end{array}\right] + \omega_r \left\{ \frac{d}{d\sigma} \left[\begin{array}{c|c} \underline{\mathrm{L}_{ss}} & \underline{\mathrm{L}_{sr}} \\ \hline \underline{\mathrm{L}_{sr}^T} & \underline{\mathrm{L}_{rr}} \end{array}\right] \right\} \left[\begin{array}{c} \underline{I_{ABC}} \\ \hline \underline{I_{abc}} \end{array}\right] \quad (2)$$

In equation (1), the first term on the right hand side represents the ohmic voltage drop in the machine windings. The second term represents the transformer voltage components, and the third term represents the rotational voltage components.

The set of state equations given in equation (1) can be represented, using the methods of reference [9], by an equivalent circuit model as shown in Figure (4). This equivalent network yields a set of differential equations which is identical to the state model given in equation (1), and hence, it is a full representation of the induction machine. Based on the state model given in equation (1), the rotational voltage components are represented in the equivalent network by the current controlled voltage sources, e_A, e_B, e_C, e_a, e_b, and e_c, shown in Figure (4). These current dependent voltage sources can be expressed as follows:

$$\begin{aligned} e_A = \omega_r[&(\frac{d}{d\sigma}L_{AA})i_A + (\frac{d}{d\sigma}L_{AB})i_B + (\frac{d}{d\sigma}L_{AC})i_C \\ &+ (\frac{d}{d\sigma}L_{Aa})i_a + (\frac{d}{d\sigma}L_{Ab})i_b + (\frac{d}{d\sigma}L_{Ac})i_c] \end{aligned} \quad (3)$$

$$e_B = \omega_r[(\frac{d}{d\sigma}L_{BA})i_A + (\frac{d}{d\sigma}L_{BB})i_B + (\frac{d}{d\sigma}L_{BC})i_C + (\frac{d}{d\sigma}L_{Ba})i_a + (\frac{d}{d\sigma}L_{Bb})i_b + (\frac{d}{d\sigma}L_{Bc})i_c] \quad (4)$$

$$e_C = \omega_r[(\frac{d}{d\sigma}L_{CA})i_A + (\frac{d}{d\sigma}L_{CB})i_B + (\frac{d}{d\sigma}L_{CC})i_C + (\frac{d}{d\sigma}L_{Ca})i_a + (\frac{d}{d\sigma}L_{Cb})i_b + (\frac{d}{d\sigma}L_{Cc})i_c] \quad (5)$$

$$e_a = \omega_r[(\frac{d}{d\sigma}L_{aA})i_A + (\frac{d}{d\sigma}L_{aB})i_B + (\frac{d}{d\sigma}L_{aC})i_C + (\frac{d}{d\sigma}L_{aa})i_a + (\frac{d}{d\sigma}L_{ab})i_b + (\frac{d}{d\sigma}L_{ac})i_c] \quad (6)$$

$$e_b = \omega_r[(\frac{d}{d\sigma}L_{bA})i_A + (\frac{d}{d\sigma}L_{bB})i_B + (\frac{d}{d\sigma}L_{bC})i_C + (\frac{d}{d\sigma}L_{ba})i_a + (\frac{d}{d\sigma}L_{bb})i_b + (\frac{d}{d\sigma}L_{bc})i_c] \quad (7)$$

$$e_c = \omega_r[(\frac{d}{d\sigma}L_{cA})i_A + (\frac{d}{d\sigma}L_{cB})i_B + (\frac{d}{d\sigma}L_{cC})i_C + (\frac{d}{d\sigma}L_{ca})i_a + (\frac{d}{d\sigma}L_{cb})i_b + (\frac{d}{d\sigma}L_{cc})i_c] \quad (8)$$

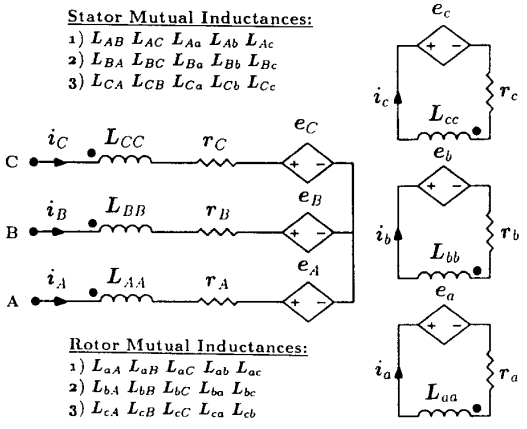

EQUIVALENT NETWORK MODEL OF INDUCTION MACHINE

Figure (4)

Here, the developed electromagnetic power of the machine is given by [13]:

$$P_{em} = e_A i_A + e_B i_B + e_C i_C \quad (9)$$

and the corresponding developed electromagnetic torque is accordingly given by:

$$T_{em} = P_{em}/\omega_m = (e_A i_A + e_B i_B + e_C i_C)/\omega_m \quad (10)$$

where, ω_m is the angular speed of the rotor in mechanical rad/s, which can be expressed as follows:

$$\omega_m = \omega_r/(p/2) = (1-s)\omega_s/(p/2) \quad (11)$$

Here, p is the number of poles.

The equivalent network of the induction machine, Figure (4), was utilized in conjunction with the power conditioner system shown in Figure (1) to obtain a global equivalent network model of the dc source-inverter fed induction motor system as shown in Figure (5). In this equivalent network model, the switching action of each diode and transistor associated with the inverter network was simulated using the same successful approach previously employed in the work of reference [4] through [7]. As depicted in Figure (5), the assumed directions of positive branch currents are shown by arrows, which are in accordance with the consumer system of notation. The state model which governs the dynamic behavior of the equivalent network of the dc source-inverter fed induction motor system, Figure (5), was automatically formulated using network graph techniques, and the hybrid-matrix representation of non-linear networks [7,14].

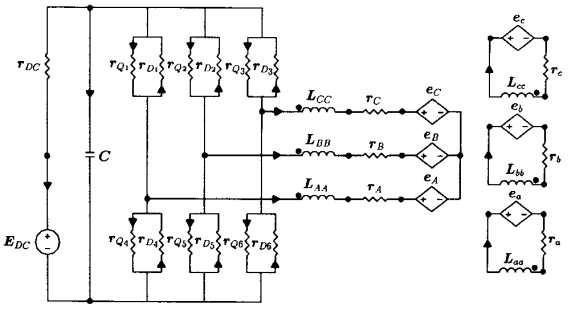

EQUIVALENT NETWORK MODEL OF DC SOURCE-INVERTER FED INDUCTION MOTOR SYSTEM

Figure (5)

For the case of squirrel cage induction motors, in which it is the practice to represent the rotor's cage by two equivalent windings, d and q, along the direct and quadrature axes of the rotor, the d and q equivalent windings replace the rotor's a, b, and c windings in equations (1) through (8). For details on this aspect, reference [15] should be consulted.

DERIVATION OF ABC EQUIVALENT NETWORK MODEL PARAMETERS FROM CONVENTIONAL INDUCTION MOTOR EQUIVALENT CIRCUITS

The main objectives of this paper are to show that this modeling approach is compatible with the conventional assumption of sinusoidally distributed mmfs and flux densities around the airgap circumference, and that the machine parameters in the ABC frame of reference are compatible with those obtained from conventional no-load and blocked rotor tests of induction machines. Again, in later papers the same model and formulation will be used to study the effects of space harmonics on machine parameters and performance characteristics.

Accordingly, in the work at hand, using the conventional symbolisms of reference [13], the machine parameters in the ABC frame of reference can be written as follows:

$$r_A = r_B = r_C = r_s \quad (12)$$

$$r_a = r_b = r_c = r_r \quad (13)$$

$$L_{AA} = L_{BB} = L_{CC} = L_{ss} \quad (14)$$

$$L_{AB} = L_{BC} = L_{CA} = L_{sm} \quad (15)$$

$$L_{aa} = L_{bb} = L_{cc} = L_{rr} \quad (16)$$

$$L_{ab} = L_{bc} = L_{ca} = L_{rm} \quad (17)$$

$$L_{Aa} = L_{Bb} = L_{Cc} = L_{srm}\cos(\sigma) \quad (18)$$

$$L_{Ab} = L_{Bc} = L_{Ca} = L_{srm}\cos(\sigma + \tfrac{2\pi}{3}) \quad (19)$$

$$L_{Ac} = L_{Ba} = L_{Cb} = L_{srm}\cos(\sigma + \tfrac{4\pi}{3}) \quad (20)$$

These parameters can also be shown to be related to the conventional shorted T-equivalent circuit of the induction motor, Figure (6), by the following relationships:

$$r_r = r'_r/a^2 \quad (21)$$

$$L_{ss} = L_{1s} + (2/3)L_m \quad (22)$$

$$L_{sm} = -(1/3)L_m \quad (23)$$

$$L_{rr} = (1/a^2)[L'_{1r} + (2/3)L_m] \quad (24)$$

$$L_{rm} = -(1/3a^2)L_m \quad (25)$$

$$L_{srm} = (2/3a)L_m \quad (26)$$

where:

r_s = stator phase resistance
L_{1s} = stator phase leakage inductance
r'_r = rotor phase resistance referred to stator
L'_{1r} = rotor phase inductance referred to stator
L_m = magnetizing inductance
s = rotor slip

For details on these relationships, references [9,15] should be consulted. Accordingly, all the parameters of the developed ABC frame equivalent network model of Figure (5) have been defined in terms of conventional induction motor circuit parameters. Next, experimental verification of the developed model is given.

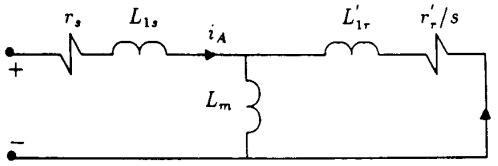

PER-PHASE CONVENTIONAL INDUCTION MOTOR EQUIVALENT CIRCUIT REFERRED TO STATOR

Figure (6)

EXPERIMENTAL VERIFICATION AND APPLICATIONS OF THE DEVELOPED MODEL

In order to experimentally verify the validity of the developed modeling technique, the global time-domain network model of the dc source-inverter fed motor system, Figure (5) was applied to a 3-phase, 204 V, 1/3 hp, 60 Hz, 4-pole induction motor fed by a dc source-inverter bridge with a conduction period of 180° electrical. This motor's equivalent circuit parameters are given in Appendix (A). The machine was tested in the laboratory to obtain its performance at various operating conditions. These operating conditions, test #1 through #3, are given in Table (1). Also, the developed global network model, Figure (5), was used to simulate the performance of the system under the same test operating conditions.

Table 1: Motor-Inverter System Test Conditions

Test #	Frequency (Hz)	Rotor Speed (RPM)	Dc Supply (Volts)
1	60	1788	150
2	60	1720	150
3	50	1470	135

For the load conditions of test #1 (no load case), the oscillogram and the corresponding computer simulated waveform (CSWF) of the machine's phase current are shown in Figures (7) and (8), respectively. Also, the oscillogram and the corresponding CSWF of the machine's line to line voltage are shown in Figures (9) and (10),respectively.

For the load conditions of test #2, the oscillogram and the corresponding CSWF of the machine's phase current are shown in Figures (11) and (12), respectively. Also, under the same operating conditions, the profile of the instantaneous developed electromagnetic torque of the machine is shown in Figure (13), and as expected, it includes torque ripples due to the nonsinusoidal nature of the ac phase currents and voltages.

For the load conditions of test #3, the oscillogram and corresponding CSWF of the machine's phase current are shown in Figures (14) and (15), respectively, and the profile of the instantaneous developed electromagnetic torque of the machine is shown in Figure (16).

Meanwhile, a comparison between actual test and simulation results for the phase current and line to line voltage magnitudes, as well as a comparison between the test and simulation results of the developed average electromagnetic torque, for the three tests #1 through #3, are given in Table (2).

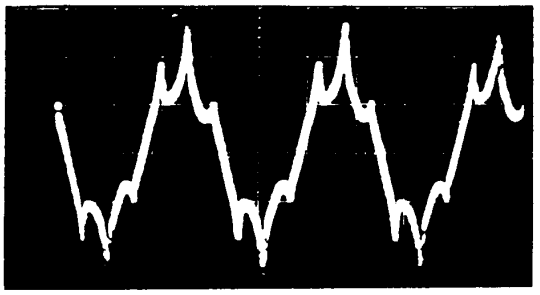

Oscillogram of Machine Phase Current
Test #1: No-load, Rotor Speed = 1788 rpm
[Horizontal: 5ms/div., Vertical: 0.5 A/div.]
Peak Value = 1.4 Amps.

Figure (7)

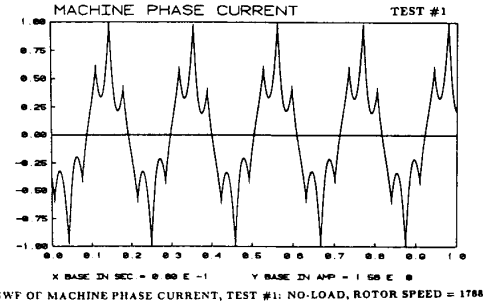

CSWF OF MACHINE PHASE CURRENT, TEST #1: NO-LOAD, ROTOR SPEED = 1788 RPM

Figure (8)

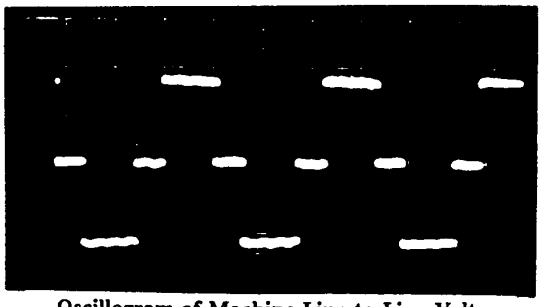

Oscillogram of Machine Line to Line Voltage
Test #1: No-load, Rotor Speed = 1788 rpm
[Horizontal: 5ms/div., Vertical: 100 V/div.]
Peak Value = 150 Volts.

Figure (9)

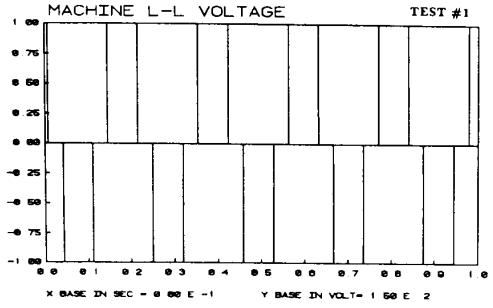

CSWF OF MACHINE L-L VOLTAGE, TEST #1: NO-LOAD, ROTOR SPEED = 1788 RPM

Figure (10)

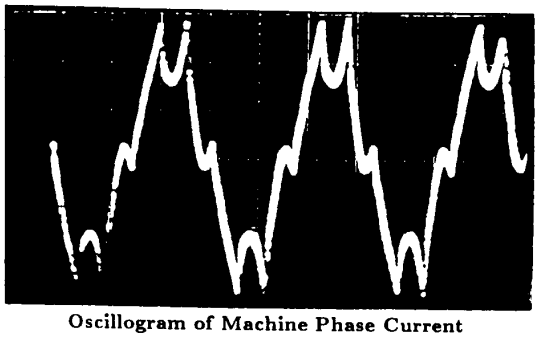

Oscillogram of Machine Phase Current
Test #2: Rotor Speed = 1720 rpm
[Horizontal: 5ms/div., Vertical: 0.5 A/div.]
Peak Value = 1.5 Amps.

Figure (11)

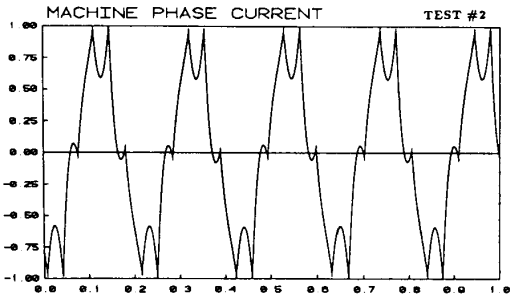

CSWF OF MACHINE PHASE CURRENT, TEST #2: ROTOR SPEED = 1720 RPM

Figure (12)

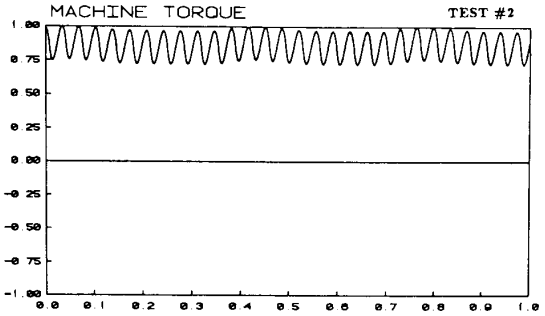

SIMULATED TORQUE PROFILE, TEST #2: ROTOR SPEED = 1720 RPM

Figure (13)

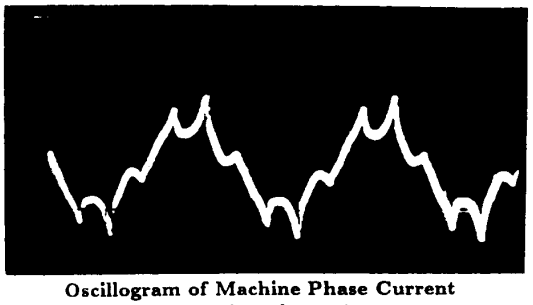

Oscillogram of Machine Phase Current
Test #3: Rotor Speed = 1470 rpm
[Horizontal: 5ms/div., Vertical: 1 A/div.]
Peak Value = 1.6 Amps.

Figure (14)

Examination of the above results including Table (2) reveals very good agreements in profile between actual and predicted waveforms, and very good agreements between measured and numerically obtained quantities, including average developed torques. It should be pointed out that such agreements between test and simulation results are harder to achieve in drives of small power ratings such as the motor at hand. However, the small horsepower rating of this drive system proved to be no hindrance to producing very good agreements between hardware test data and simulation results. Hence, these results demonstrate that the developed model in the ABC frame of reference has the ability to predict the dynamic performance of this class of dc source-inverter fed induction motor systems for larger ratings and load conditions. Next this model will be used to investigate the effects of varying the inverter conduction period on various aspects of a 15 hp motor-inverter system performance. This motor was chosen for its compatibility in rating with other brushless dc motors studied in references [3-8].

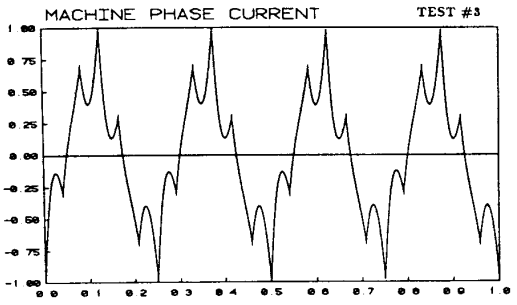

CSWF OF MACHINE PHASE CURRENT, TEST #3; ROTOR SPEED = 1470 RPM

Figure (15)

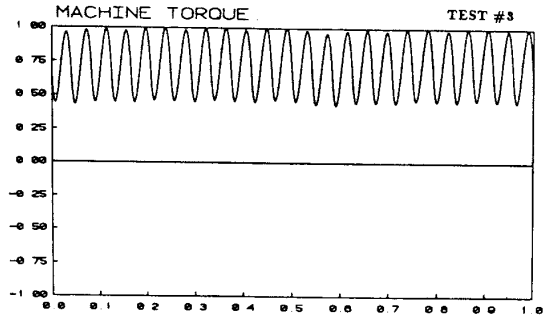

SIMULATED TORQUE PROFILE, TEST #3; ROTOR SPEED = 1470 RPM

Figure (16)

Table 2: Comparison Between Actual and Simulation Results

Test #	Quantity	Lab Test	Simulation
1	Line to Line Voltage Peak Value (Volts)	150	150
1	Phase Current Peak Value (Amps.)	1.4	1.56
2	Phase Current Peak Value (Amps.)	1.5	1.59
2	Average Torque (N.m.)	0.63	0.59
3	Phase Current Peak Value (Amps.)	1.6	1.67
3	Average Torque (N.m.)	0.28	0.26

USE OF MODEL IN EVALUATING EFFECTS OF 180° AND 120° INVERTER CONDUCTION PERIODS ON MOTOR PERFORMANCE

Conduction periods of the inverter's transistors (or SCRs) play an important role in the performance of the dc source-inverter fed induction motor systems. Since the two conduction periods, 180° e and 120° e, are widely used, it is advantageous to use the developed global equivalent network model of the motor-inverter system, Figure (5), to study the performance of such motor drive systems under these two modes of operation.

The equivalent network model of the motor-inverter system, Figure (5), was used to simulate the performance of a 3-phase, 440 V, 15 hp, 60 Hz, 8-pole wound rotor induction motor, whose equivalent circuit parameters are given in Appendix (B). The simulations were carried out under a 564 V dc voltage supply and a rotor speed of 864 rpm (slip=0.04), for the case of 180° e and 120° e inverter conduction periods.

The machine's phase current waveforms for the 180° e and 120° e conduction periods are shown in Figures (17) and (18), respectively. Examining these figures, one can notice that for the case of 120° e conduction period, the phase current is almost discontinuous during the 60° e period when the two transistors are *off*. Meanwhile, the phase current for the case of 180° e conduction period is always continuous.

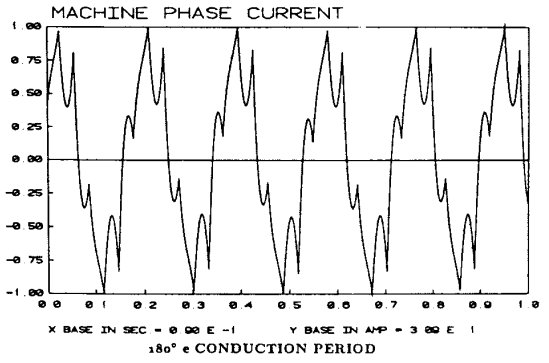

180° e CONDUCTION PERIOD

Figure (17)

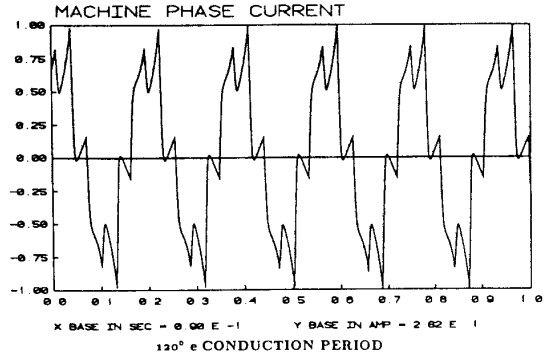

120° e CONDUCTION PERIOD

Figure (18)

The profiles for the developed electromagnetic torque of the machine for the 180° e and 120° e conduction periods are shown in Figures (19) and (20), respectively. Based on these torque profiles, it was found that for the same dc voltage supply (564 V) and the same rotor speed (864 rpm), the developed average electromagnetic output power was found to be 7.87 KW (10.55 hp) for the case of 120° e conduction period, compared to 10.22 KW (13.7 hp) for the case of 180° e conduction period. This difference in output power is expected since the fundamental ac

component of the inverter's line to line output voltage for the case of 180° e conduction period is higher in magnitude than that of the fundamental ac component for the case of 120° e conduction period. Therefore, the results of this simulation model indicate as expected that for the same input dc voltage supply, the motor-inverter system is able to deliver more output power when the inverter's transistors are operating with 180° e conduction periods. Moreover, by means of the model developed here, it was found that in order for the motor-inverter system to deliver 10.22 KW of output power for the case of 120° e conduction period, the dc voltage supply for the system has to be raised to 651 V (compared to 564 V for the case of 180° e conduction period). Armature winding insulation considerations may preclude in many instances operating such a motor at these voltage levels for any sustained (non-momentary) periods of time.

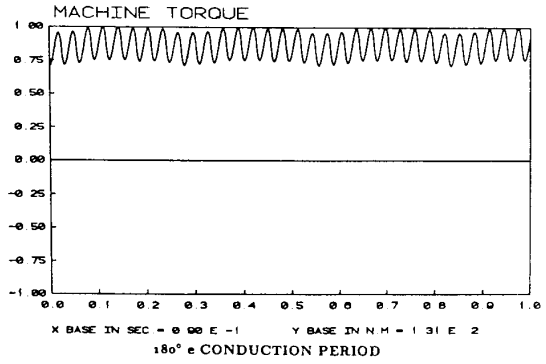

Figure (19)

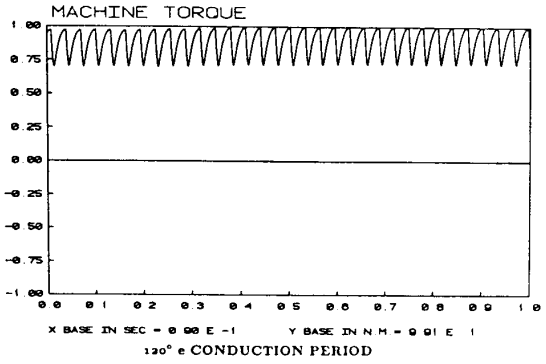

Figure (20)

CONCLUSIONS

A natural ABC frame of reference time-domain equivalent network model for the analysis of the dynamic performance of dc source-inverter fed induction motor systems was presented. Because of the fact that the formulation of the model is based on the natural ABC frame of reference, effects of space harmonics (due to rotor and stator slottings) on the machine parameters can be directly incorporated in the model's formulation as will be demonstrated in future work. A significant advantage in this approach is the fact that it readily facilitates the ability to directly link the machine's dynamic model to the equivalent circuit model of any power conditioner, and hence, it enables one to directly compare simulation results with corresponding test data, which are necessarily obtained in the natural ABC form. That is, the electronically switched currents are also the state variable currents of the machine's windings, thus avoiding "synthetic" transformed frame of reference currents, voltages etc. Furthermore, the parameters of the machine's equivalent network model were shown to be compatible with those parameters of any induction motor's conventional T-equivalent circuit obtained from no-load and blocked rotor tests.

The validity of the developed model was confirmed by applying it to the prediction of the performance of an example 204 V, 1/3 hp, 60 Hz, 4-pole induction motor-inverter system with 180° e conduction period, for which the simulation results and corresponding test data at different load conditions produced very good correlations and agreements. The model was also used to evaluate the effects of 180° e and 120° e inverter conduction periods on the performance of a 440 V, 15 hp, 60 Hz, 8-pole induction motor-inverter system, the results of which were in agreement with previous experience relating to these two conduction periods. Thus, these results further confirm the soundness of this modeling technique.

Appendix A

1/3 hp induction motor circuit parameters:

Stator	rotor
$r_s = 6.2\Omega$	$r'_r = 4.2\Omega$(referred to stator)
$L_{1s} = 18.3mH$	$L'_{1r} = 18.6mH$(referred to stator)
$L_m = 267mH$	

Appendix B

15 hp induction motor circuit parameters:

Stator	rotor
$r_s = 0.52\Omega$	$r'_r = 0.634\Omega$(referred to stator)
$L_{1s} = 3.05mH$	$L'_{1r} = 3.053mH$(referred to stator)
$L_m = 106.1mH$	

References

[1] Sawyer, B. and Edge, J.T., "Design of a Samarium-Cobalt Brushless DC Motor for Electromechanical Actuator Applications," *Proceedings of the IEEE-National Aerospace and Electronics Conference,* Dayton, Ohio, 1977.

[2] Edge, J.T., "An Electromechanical Actuator Technology Development Program," Paper No. 780581, Society of Automotive Engineers, *Proceedings of the Aerospace Fluid Power and Control Technologies Symposium,* 1978.

[3] Demerdash, N.A., Miller, R.H., Nehl, T.W., Overton, B.P., and Ford, C.J.,"Comparison Between Features and Performance Characteristics of Fifteen HP Samarium Cobalt and Ferrite Based Brushless DC Motors Operated by the Same Power Conditioner," *IEEE Transactions on Power Apparatus and Systems,* Vol. PAS-102, pp. 104-112, 1983.

[4] Hijazi, T.M. and Demerdash, N.A., "Computer-Aided Modeling and Experimental Verification of the Performance of Power Conditioner Operated Permanent Magnet Brushless DC Motors Including Rotor Damping Effects," *IEEE Transactions on Energy Conversion,* Vol. 3, No. 3, 1988, pp. 714-721.

[5] Hijazi, T.M. and Demerdash, N.A., "Impact of the Addition of a Rotor-Mounted Damper Bar Cage on the Performance of Samarium-Cobalt Permanent Magnet Brushless Dc Motor Systems," *IEEE Transactions on Energy Conversion,* Vol. 3, No. 3, 1988, pp. 890-898.

[6] Demerdash, N.A. and Nehl, T.W., "Dynamic Modeling of Brushless DC Motors For Aerospace Actuation", *IEEE Transactions on Aerospace and Electronic Systems,* Vol. AES-16, No. 6, 1980, pp. 811-821.

[7] Nehl, T.W., Demerdash, N.A., Hijazi, T.M., and McHale, T.L., "Automatic Formulation of Models for Simulation of the Dynamic Performance of Electronically Commutated DC Machines", *IEEE Transactions on Power Apparatus and Systems,* Vol. PAS-104, No. 8, 1985, pp. 2214-2222.

[8] Demerdash, N.A., Hijazi, T.M., and Arkadan, A.A., "Computation of Winding Inductances of Permanent Magnet Brushless DC Motors with Damper Windings by Energy Perturbation," *IEEE Transactions on Energy Conversion,* Vol. 3, No. 3, 1988, pp. 705-713.

[9] Krause, P.C. and Lipo, T.A., "Analysis and Simplified Representations of a Rectifier-Inverter Induction Motor Drive," *IEEE Transactions on Power Apparatus and Systems,* Vol. PAS-88, pp. 588-596, 1969.

[10] Cornell, E.P. and Lipo, T.A., "Modeling and Design of Controlled Current Induction Motor Drive Systems," *IEEE Transactions on Industry Applications,* Vol. IA-13, pp.321-330, 1977.

[11] Arkadan,A.A.,Demerdash,N.A., Vaidya,J.G., and Shah,M.J. "Impact of Load on Winding Inductances of Permanent Magnet Generators with Multiple Damping Circuits Using Energy Perturbation", *IEEE Transactions on Energy Conversion,* Vol. 3, No. 4, 1988, pp. 880-889

[12] Arkadan,A.A. and Demerdash,N.A.,"Modeling of Transients in Permanent Magnet Generators with Multiple Damping Circuits Using the Natural abc Frame of Reference", *IEEE Transactions on Energy Conversion,* Vol. 3, No. 3, 1988, pp. 722-731

[13] Fitzgerald, A.E. and Kingsly, Jr., Charles, *Electric Machinary,* Second Edition, McGraw-Hill Book Company Inc., 1961.

[14] Chua, L.O., and Lin, P.M., *Computer-Aided Analysis of Electrical Circuits: Algorithms and Computational Technique*, New Jersey: Prentice-Hall, Inc. 1975.

[15] Alhamadi, M.A., "Modeling and Analysis of Inverter-Fed Induction Motors Using the Natural ABC Frame of Reference and Network Graph Techniques," M.Sc. Thesis, *Clarkson University,* May 1988.